DENTAL MATERIALS 36 (2020) 1566–1577

Available online at www.sciencedirect.com

ScienceDirect

journal homepage: www.intl.elsevierhealth.com/journals/dema

Antimicrobial effect of nanostructured membranes for guided tissue regeneration: an *in vitro* study

J. Bueno[a], *MC. Sánchez*[a], *M. Toledano-Osorio*[b], *E. Figuero*[a], *M. Toledano*[b], *AL. Medina-Castillo*[c], *R. Osorio*[b,*], *D. Herrera*[a], *M. Sanz*[a]

[a] *ETEP (Etiology and Therapy of Periodontal Diseases) Research Group, University Complutense, Madrid, Spain*
[b] *Biomaterials in Dentistry Research Group, University of Granada, Spain*
[c] *NanoMyP. Spin-Off Enterprise from University of Granada, Edificio BIC-Granada, Av. Innovación 1. 18016 Armilla, Granada, Spain*

ARTICLE INFO

Keywords:
Calcium
Doxycycline
Periodontology
Guided tissue regeneration
Nanostructured membranes
Antimicrobial membranes
Nanotechnology
Biofilm model
Nanopolymers
Scaffolds

ABSTRACT

Objective. The purpose of this *in vitro* study was to evaluate the antibacterial effect of a novel non-resorbable, bioactive polymeric nanostructured membrane (NMs), when doped with zinc, calcium and doxycycline.

Methods. A validated *in vitro* subgingival biofilm model with six bacterial species (*Streptococcus oralis, Actinomyces naeslundii, Veillonela parvula, Fusobacterium nucleatum, Porphyromonas gingivalis* and *Aggregatibacter actinomycetemcomitans*) was used. The experimental NMs, with and without being doped with doxycycline, calcium and zinc, were placed on hydroxyapatite (HA) discs. As positive control membranes, commercially available dense polytetrafluoroethylene (d-PTFE) membranes were used and, as negative controls, the HA discs without any membrane. The experimental, positive and negative control discs were exposed to a mixed bacterial suspension, at 37 °C under anaerobic conditions, during 12, 24, 48 and 72 h. The resulting biofilms were analyzed through scanning electron microscopy (SEM), to study their structure, and by quantitative polymerase chain reaction (qPCR), to assess the bacterial load, expressed as colony forming units (CFU) per mL. Differences between experimental and control groups were evaluated with the general linear model and the Bonferroni adjustment.

Results. As shown by SEM, all membrane groups, except the NMs with doxycycline, resulted in structured biofilms from 12–72 hours. Similarly, only the membranes loaded with doxycycline demonstrated a significant reduction in bacterial load during biofilm development, when compared with the control groups ($p < 0.001$).

Significance. Doxycycline-doped nanostructured membranes have an impact on biofilm growth dynamics by significant reducing the bacterial load.

* Corresponding author at: Dental School, University of Granada, Colegio Máximo, Campus de Cartuja s/n 18017 Granada, Spain.
E-mail address: rosorio@ugr.es (R. Osorio).

https://doi.org/10.1016/j.dental.2020.09.011
0109-5641/

1. Introduction

Periodontitis is a chronic inflammatory disease associated with bacterial dysbiosis and characterized by progressive destruction of the tooth-supporting structures [1]. Severe periodontitis, the form with the highest morbidity, is the sixth most frequent disease worldwide, affecting 11.2% of the population [2]. This disease not only can lead to tooth loss, but has a relevant impact on quality of life [3] and may influence the incidence and progression of different systemic diseases [4], and even overall death [5]. While the aetiology of this chronic inflammatory disease is multifactorial, subgingival bacteria organised in biofilms are accepted as the primary etiological factor [6–9].

The treatment of periodontitis is mainly based on infection control measures, by mechanically disrupting and reducing the sub-gingival bacterial biofilm [10–12]. In specific periodontal lesions (intrabony defects), however, different regenerative treatments have shown the ability to regenerate the periodontal attachment apparatus, although this outcome is not always predictable [13–18]. Among these regenerative technologies, guided tissue regeneration (GTR), based on the concept of tissue compartmentalization and homing, has demonstrated the achievement of periodontal regenerative outcomes [19,20], although these were often compromised by bacterial colonization and infection, mainly when these barrier membranes were exposed [21–24]. Hence, a new generation of barrier membranes with enhanced properties is being developed. Among these, nanostructured membranes have been proposed due to their ability to enhance cell adhesion, migration, proliferation and cell differentiation, thus promoting regenerative outcomes [16,17,25–30]. Furthermore, the presence of carboxylic groups (COOH) on their surface [16] allows for the ability to chelate metal ions and other substances, such as antibiotics, conferring these biomaterials with antimicrobial properties. Metal cations, such as zinc and calcium, have shown certain antibacterial effect [31,32] and the use of doxycycline has shown multiple beneficial effects beyond its antimicrobial activity [33,34].

It was, therefore, the aim of this *in vitro* investigation, to evaluate the antibacterial activity of a biocompatible, non-resorbable polymeric and nanostructured membrane [16], with and without doping agents (zinc, calcium or doxycycline), and to compare it with positive and negative control membranes, using a validated multi-species subgingival biofilm model.

2. Materials and methods

2.1. Bacterial strains and culture conditions

The following reference strains were used: *Streptococcus oralis* CECT 907 T, *Veillonella parvula* NCTC 11810, *Actinomyces naeslundii* ATCC 19039, *Fusobacterium nucleatum* DMSZ 20482, *Aggregatibacter actinomycetemcomitans* DSMZ 8324 and *Porphyromonas gingivalis* ATCC 33277. These bacteria were grown on blood agar plates (Blood Agar Oxoid Nº 2; Oxoid, Basingstoke, UK), supplemented with 5% (v/v) sterile horse blood (Oxoid), 5.0 mg L^{-1} hemin (Sigma, St. Louis, MO, USA) and 1.0 mg L^{-1} menadione (Merck, Darmstadt, Germany) under anaerobic conditions (10% H_2, 10% CO_2, and balance N_2) at 37 °C for 24–72 hours.

2.2. Nano-structured membrane technology

Nano-structured membranes (NMs) were fabricated by electrospinning, using a novel polymeric blend (PolymBlend®, NanoMyP, Granada, Spain) optimized for the production of non-woven nanofiber mats. Novel membranes were fabricated by electrospinning with a mixture of (MMA)1-co-(HEMA)1 and (MA)3-co-(HEA)2. Electrospun fibers at NMs are randomly distributed and have a diameter of approximately 300 nm. Micro- and nano-pores are found between fibers, resembling the collagen structure of human bone [16]. The membrane surface was modified by chemical functionalization and doped with calcium (Ca-NM), zinc (Zn-NM) or doxycycline (Dox-NM). This was done by pre-activating the NMs with a sodium carbonate buffer solution (333 mM; pH = 12.5) for 2 h and then washed with water, what resulted in the partial hydrolysis of the ester bonds and carboxyl groups on the surface. Surfaces were later doped by incubating the NMs with different aqueous solutions of CaCl2, ZnCl2 (containing zinc or calcium at 40 ppm, for 3 days) (pH 6.5) or doxycycline (40 mg ml-1 of doxycycline hyclate, during 4 h) at room temperature with continuous shaking [16]. Morphology, topography and NMs structure were not altered after doping [16]. The commercially available control membrane (Cytoplast®, Osteogenic Biomedical, Lubbock, TX, USA) is made of dense polytetrafluoroethylene (d-PTFE). These membranes are not nanostructured, but they are arranged in symmetrical rows of regular hexagons with sides 200 microns long, separated one to the other about 0.5 mm.

2.3. Sample preparation

Calcium hydroxyapatite (HA) discs of 7 mm in diameter and 1.8 mm in thickness (standard deviation, SD = 0.2) (Clarkson Chromatography Products, Williamsport, PA, USA) were covered with the tested NMs and also with the positive control membranes made of dense polytetrafluoroethylene (d-PTFE) (Cytoplast®, Osteogenic Biomedical, Lubbock, TX, USA). As negative control, the HA discs were coated with phosphate buffer saline (PBS) without any barrier membrane.

2.4. Biofilm model

Pure cultures of each bacterium which were grown anaerobically in brain-heart infusion (BHI) (Becton, Dickinson and Company, Franklin Lakes, NJ, USA) culture medium supplemented with 2.5 g L^{-1} mucin (Oxoid), 1.0 g L^{-1} yeast extract (Oxoid), 0.1 g L^{-1} cysteine (Sigma), 2.0 g L^{-1} sodium bicarbonate (Merck), 5.0 mg L^{-1} hemin (Sigma, St. Louis, MO, USA) and 1.0 mg L^{-1} menadione (Merck, Darmstadt, Germany) and 0.25% (v/v) glutamic acid (Sigma). At mid-exponential phase of bacterial growth (measured by spectrophotometry), a mixed bacterial suspension containing 10^3 colony forming units (CFU) mL^{-1} of *S. oralis*, 10^5 CFU mL^{-1} of *V. parvula* and *A. naeslundii*, and 10^6 CFU mL^{-1} of *F. nucleatum, A. actinomycetemcomitans* and *P. gingivalis* was prepared.

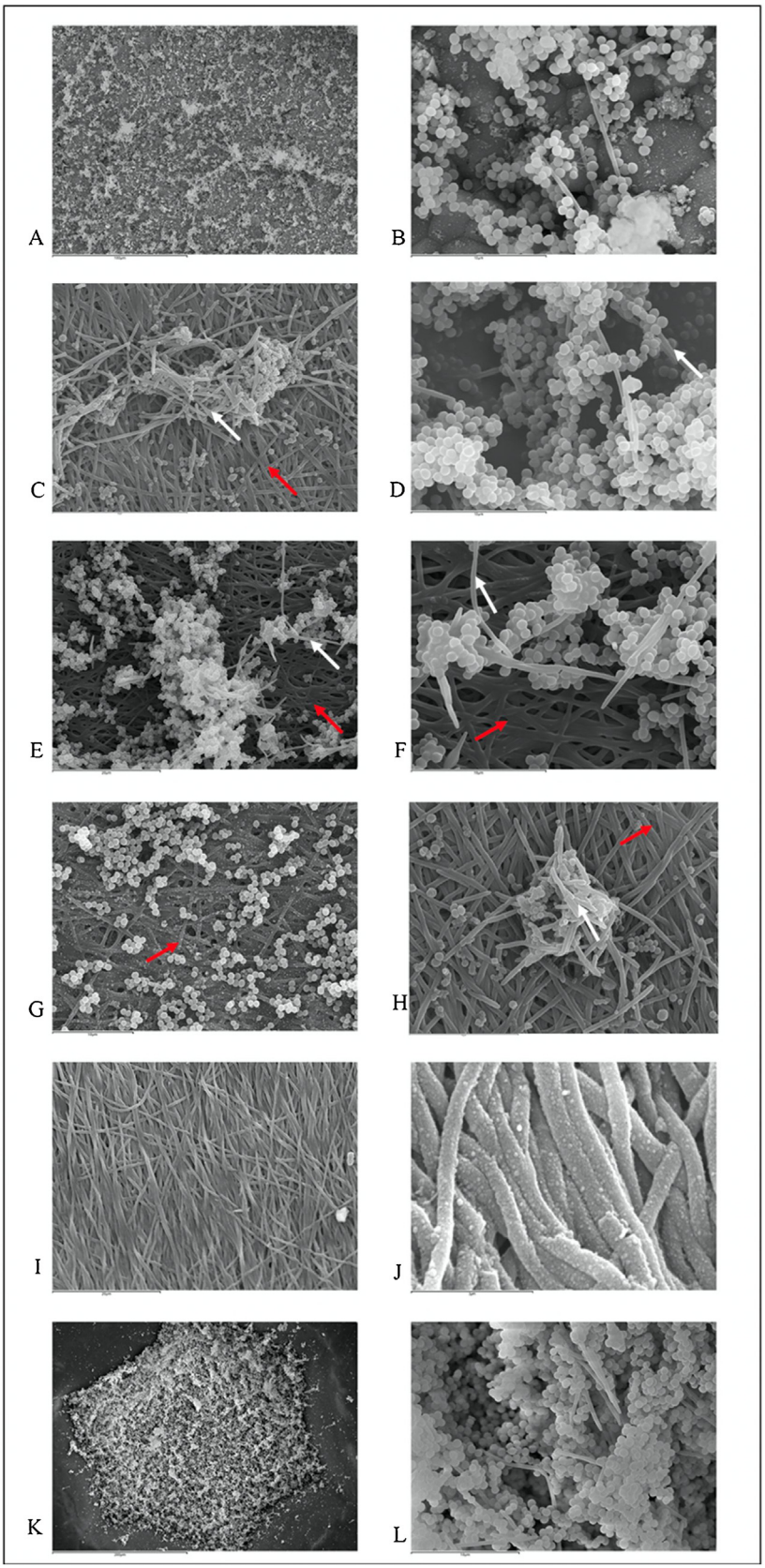

Fig. 1 – Scanning Electron Microscopy images of biofilms after 12 h on [(A) and (B)]) hydroxyapatite discs; [(C) and (D)] nanostructured membranes (NMs); [(E) and (F)] calcium NMs; [(G) and (H)] zinc NMs; [(I) and (J)] doxycycline NMs; [(K) and (L)] dense polytetrafluoroethylene (d-PTFE). Bacterial cells are disposed as individual or grouped cells onto the surfaces, except for doxycycline NMs, where bacteria are not evidenced onto the surfaces (I and J) and on d-PTFE membranes where the

HA discs covered with either NMs (NMs, Zn-NMs, Ca-NMs and Dox-NMs), positive (d-PTFE) and negative control discs were located in the wells of a 24-well tissue culture plate (Greiner Bio-one, Frickenhausen, Germany), and 1.5 mL of the mixed bacterial suspension were spilled in each well. Plates were incubated in anaerobic conditions at 37 °C for 12, 24, 48 and 72 h. To control for appropriate sterility, plates containing only culture medium were also incubated.

2.5. *Biofilms structural analysis with scanning electron microscopy (SEM) and energy dispersion X-Ray (EDX)*

The resulting 12–72 hours biofilms were studied by SEM. The SEM processing of the discs included, first, fixation with a solution of 4% paraformaldehyde and 2.5% glutaraldehyde for 4 h at 4 °C, then washing in PBS, then in sterile water for 10 min and dehydrated through a series of graded ethanol solutions (30, 50, 70, 80, 90 and 100%; immersion time per series 10 min). Once dried by critical point, the discs were sputter-coated with gold and analysed with a SEM with a back-scattered electron detector and an image resolution of 25 kV (JSM6400; JEOL, Tokyo, Japan). In selected specimens, Energy Dispersion X-Ray (EDX) (JSM6400; JEOL, Tokyo, Japan) was also used.

2.6. *Bacterial analysis by quantitative polymerase chain reaction (qPCR)*

Cultured HA discs, with or without membranes, were collected in sterile tubes with 1 mL of PBS. The bacterial samples were collected through vigorous shaking with vortex for 3 min in order to optimize DNA bacterial collection from the biofilm samples [35]. DNA of 12, 24, 48- and 72 -hs growth biofilms was isolated using a commercial kit, following manufacturer's instructions (MolYsis Complete5; Molzym GmgH & CoKG, Bremen, Germany), and then quantified using the hydrolysis probe 5ńuclease assay qPCR method with specific primers for the six bacterial species used. These primers and probes [obtained by Life Technologies Invitrogen (Carlsbad, CA, USA) and Roche (Roche Diagnostic GmbH; Mannheim, Germany)] were targeted against 16S rRNA gene [35]. The qPCR amplification was performed in a total reaction mixture volume of 10 μL. The reaction mixtures contained 5 μL of 2x master mixture (LC 480 Probes Master; Roche), optimal concentrations of primers and probe (900, 900 and 300 nM for *S. oralis*; 300, 300 and 300 nM for *A. naeslundii*; 750, 750 and 400 nM for *V. parvula*; 300, 300 and 200 nM for *A. actinomycetemcomitans*; 300, 300 and 300 nM, for *P. gingivalis* and 600, 600 and 300 nM for *F. nucleatum*), and 2 μL of DNA from samples. The negative control was 2 μL of sterile water [no template control (NTC)] (Water PCR grade, Roche). The samples were subjected to an initial amplification cycle of 95 °C for 10 min, followed by 45 cycles at 95 °C for 15 s and 60 °C for 1 min. Analyses were performed with a LightCycler® 480 II thermocycler (Roche). LightCycler® 480 Multiwell Plates 384 and sealing foils were used (Roche).

Each DNA sample was analyzed in duplicate. Quantification cycle (Cq) was determined using the provided software package (LC 480 Software 1.5; Roche). Quantification of cells by qPCR was based on standard curves. The correlation between Cq values and CFU mL^{-1} were automatically generated through the software (LC 480 Software 1.5; Roche).

2.7. *Statistical analysis*

Data were expressed as means and SD. The distribution and normality were tested by the Shapiro–Wilk goodness-of-fit tests. To compare the antimicrobial effects of the tested materials on the disc (bacterial load expressed on CFU mL^{-1}), a general lineal model was constructed for each bacterial species (*S, oralis, A. naeslundii, V. parvula, A. actinomycetemcomitans, P. gingivalis* and *F. nucleatum*) and for the total bacteria using the method of maximum likelihood and Bonferroni corrections for multiple comparisons. Results were considered statistically significant at $p < 0.05$. A software package (IBM SPSS Statistics 22.0; IBM Corporation, Armonk, NY, USA) was used for all data analysis.

3. Results

3.1. *Structural analysis of biofilms by SEM/EDX*

After 12 h of biofilm development, the HA discs not covered with a barrier membrane showed presence of bacteria on their surface as individual cells, bacterial chains, and multicellular mixed colonies (cell to cell coaggregation). Fusiform bacilli (corresponding to *F. nucleatum*) could be observed forming a three-dimensional net, with different morphotypes of bacteria adhered to their surface (Fig. 1A-B). Twelve-hour biofilms on discs covered with NMs, Ca-NM_S and Zn-NMs membranes, showed a similar bacterial biomass and structural organization as those formed on HA discs not covered with membranes (negative control) (Fig. 1 C-H). The positive control discs, covered with d-PTFE membranes, showed similar biomass of bacteria although with a particular colonization pattern (Fig. 1 K-L), forming a regular hexagon lattice architecture (Fig. 2). After 12 h of biofilm growth, only the discs doped with doxycycline (Dox-NMs) demonstrated statistically significant differences, in terms of biomass and structure, since the presence of bacteria was hardly observed over the membrane surface (Fig. 1 I-J).

After 24 h, the amount of the biofilm increased with the presence of bacterial colonization covering the entire disc area on test (NMs, Ca-NMs and Zn-NMS) and control discs, always with a similar biofilm structure. Only in the discs covered with Dox-NMs, biofilm formation was clearly reduced (Fig. 3 A). In the positive control discs, the resulting biofilms maintained

growth of bacteria was produced inside the wells of the membrane (K and L). Spindle-shaped rods cells compatible with *F. nucleatum* could be recognized, being an important part of the connection between the different bacteria (white arrows). The NMs surface is sometimes visible (red arrows). Magnification: (A) 500X; (B, D) 5000X; (C) 2500X; (E) 2000X; (F) 5000X; (G) 3000X; (H) 4000X (I) 2000X; (J) 15000X (K) 250X; (L) 4000 × .

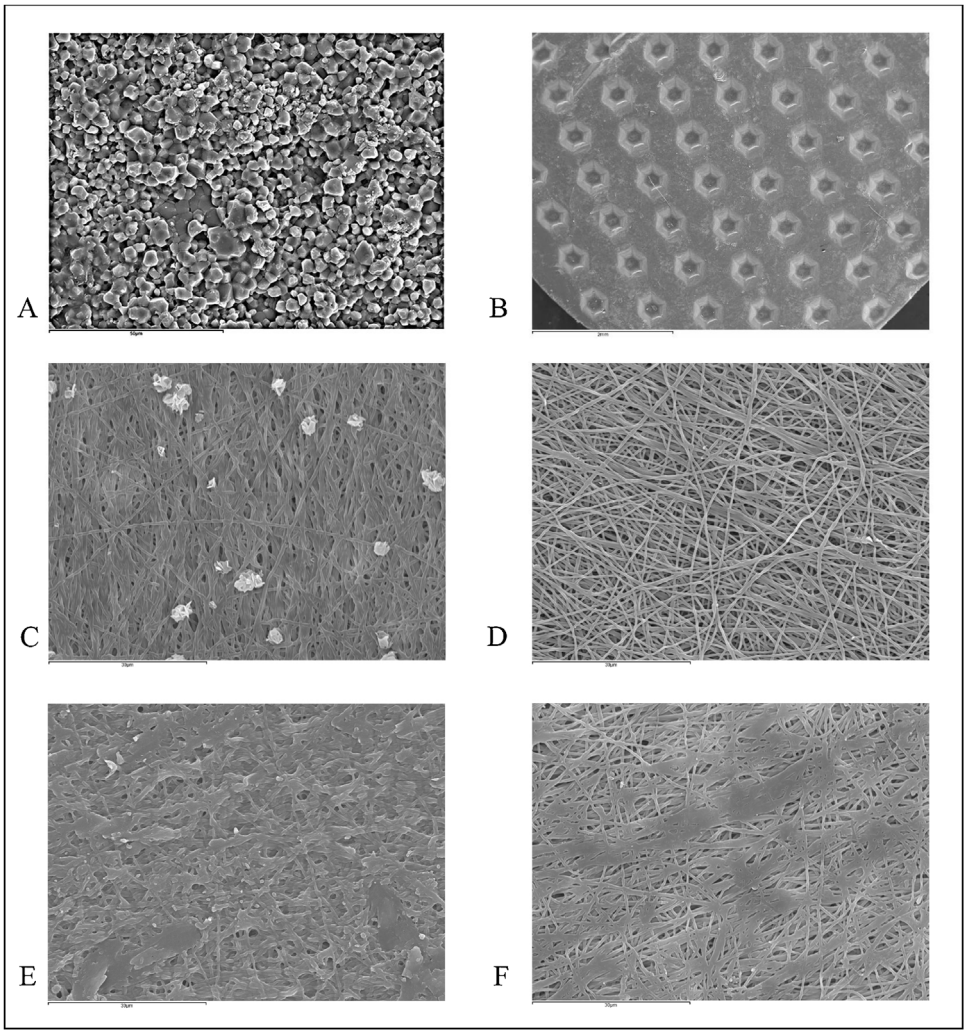

Fig. 2 – Scanning Electron Microscopy images of membranes on (A) hydroxyapatite discs; (B) dense polytetrafluoroethylene (d-PTFE); (C) nanostructured membranes (NMs); (D) calcium NMs; (E) zinc NMs; and (F) doxycycline NMs. Magnification: (A) 1000X; (B, C, D, E, F) 1500 × .

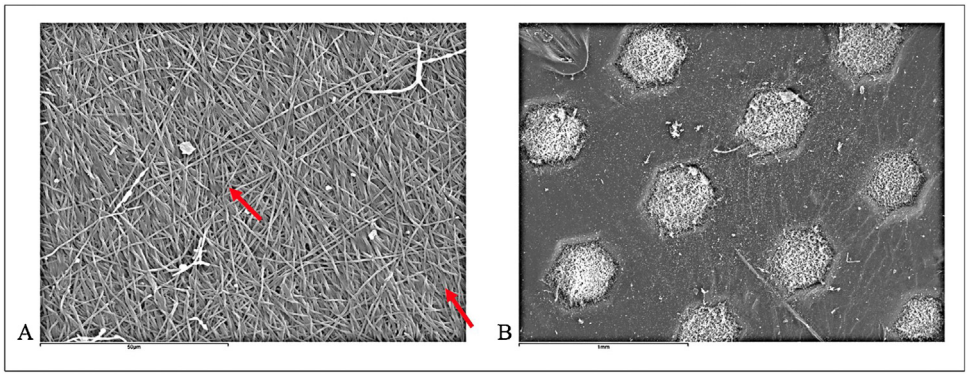

Fig. 3 – Scanning Electron Microscopy images of biofilms after 24 h of development on (A) nanostructured membranes (NMs) with doxycycline; (B) dense polytetrafluoroethylene (d-PTFE). The number of bacteria grew in all groups except for doxycycline NMs, where only a few cells could be observed over the membrane, probably dead or detached. At picture B, the growth of the bacteria occurred inside the wells of d-PTFE membranes. Some minerals precipitation is detected (A) (red arrows). Magnification: (A), 1,000X; (B), 45 × .

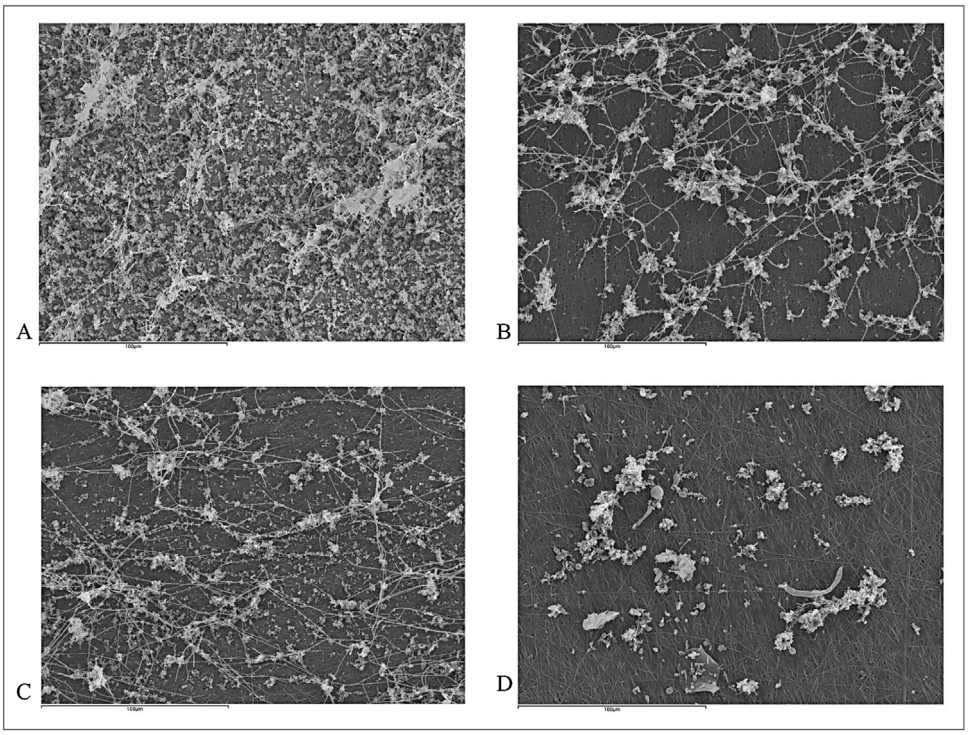

Fig. 4 – Scanning Electron Microscopy images of biofilms after 48 h of development on (A) hydroxyapatite discs; (B) nanostructured membranes (NMs) with calcium; (C) zinc NMs; (D) doxycycline NMs. The bacterial load is reduced in calcium, zinc or doxycycline loaded NMs. Magnification: 500 × .

the influence of this membrane structure (Fig. 3 B). After 48 h, all discs covered with NMs demonstrated a decreased bacterial mass when compared with negative (HA) and positive (d-PTFE) control discs (Fig. 4).

After 72 h, a thick layer of bacteria covered all specimens, with *F. nucleatum* representing the most noticeable bacterial species, surrounded by multiple bacterial micro-colonies (Fig. 5

), acquiring the typical biofilm-structure on all tested membranes, with presence of bacterial organised in stacks and tunnels for nutrient circulation (Fig. 5). These biofilms were completely mature in all tested groups excepted on Dox-NMs, with a significantly reduced bacterial load and a structure of a poorly structured biofilm (Fig. 5 I-J). In these 72 -hs biofilms, EDX analysis confirmed the presence of mineral deposits of calcium and sodium salts on the membrane surface (Supplementary Fig. 1).

3.2. *Quantitative evolution of the bacterial load and presence of specific bacteria*

Table 1 depicts the effect of the different NMs on total bacterial counts, at different time points between 12 and 72 -hs biofilms. Until reaching the exponential phase (up to 48 h), biofilms on NMs demonstrated a lower total number of bacteria compared to control biofilms (HA discs). This effect was more noticeable in 48 -hs biofilms in contact to Ca-NMs ($p = 0.003$, as compared with negative HA control biofilms).

In mature biofilms (72 h), this effect was lost, with high numbers of bacteria present on the membrane nanofibers. Significantly higher numbers of bacteria were present on Ca-NMs and Zn-NMs when compared to positive control (d-PTFE) membranes ($p = 0.050$ and $p = 0.015$, respectively). Nevertheless, there was no statistically significant differences in the amounts of bacteria on Ca-NMs and Zn-NMs when compared with negative control HA discs ($p \leq 0.245$). Similarly, bacterial load in contact with d-PTFE membranes and NMs without charge did not significantly differ with HA discs ($p = 1.00$ in both cases).

Dox-NMs maintained the antibacterial effect at all time points during biofilm formation and maturation. In contact to doxycycline, the total bacteria load was significantly lower in the biofilms after 12, 24, 48 and 72 h, when compared to the other groups ($p < 0.001$ in all cases).

The effect of the different tested membranes on each of the bacterial species during their biofilm growth is depicted in Table 2. At 12 h, no statistically significant differences were observed among the different bacterial species growing in the tested membranes when compared with the negative control group (HA), excepted for Dox-NMs [$p \leq 0.005$ in all cases, except for *P. gingivalis* ($p \leq 0.060$)]. Within the NMs studied, statistically significant lower bacterial counts for the primary colonizers *S. oralis*, *A. naeslundii* and *V. parvula* and the secondary colonizers *F. nucleatum* and *A. actinomycetemcomitans*, were found in Dox-NMs, when compared with the other groups ($p \leq 0.005$ in all cases), except for *A. naeslundii* when compared to Zn-NMs ($p = 0.808$).

After 24 h, statistically significant lower bacterial counts for all tested bacteria were found in Dox-NMs when compared to the other groups ($p \leq 0.001$). Also, the positive control group (d-

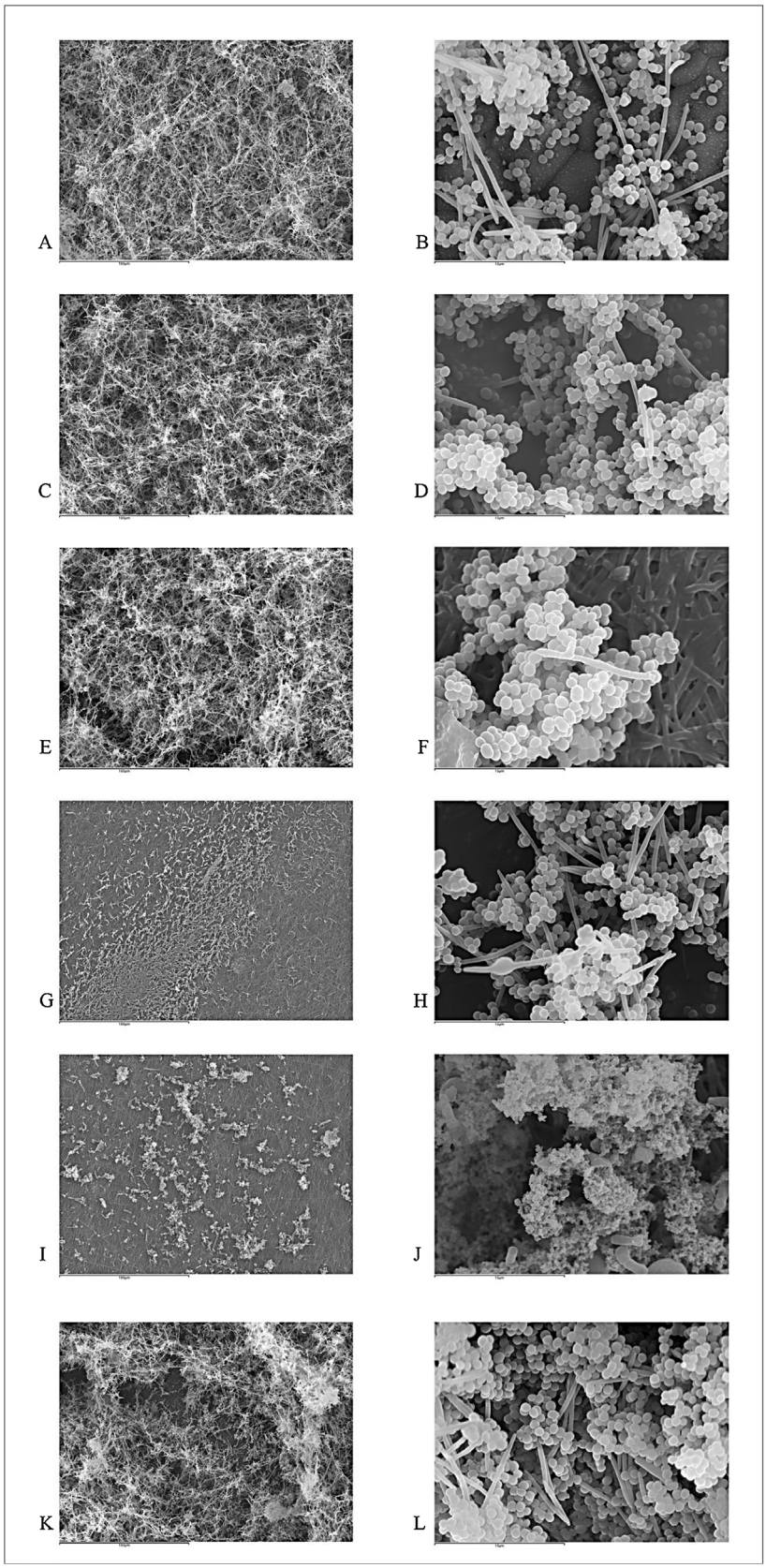

Fig. 5 – Scanning Electron Microscopy images of biofilms after 72 h of development on hydroxyapatite coated with [(A) and (B)] Phosphate Buffered Saline (PBS); [(C) and (D)] nanostructured membranes (NMs); [(E) and (F)] calcium NMs; [(G) and (H)] zinc NMs; [(I) and (J)] doxycycline NMs; [(K) and (L)] dense polytetrafluoroethylene (d-PTFE). Bacterial community acquired the typical biofilm-structure over all membranes, with the bacteria organized in stacks leaving holes for the nutrient's

Table 1 – Number of total bacteria [colony forming units (CFU)/biofilm], expressed as mean and standard deviation (SD), grown as multi-species biofilm at the different times of incubation, measured by quantitative real-time polymerase chain reaction (qPCR) (N = 3 for each incubation time and material). Hydroxyapatite discs (HA) and dense polytetrafluoroethylene d-PTFE membranes were used as controls, and four experimental nanostructured membranes (NMs) were tested: no doped active NMs, doped with calcium (Ca-NMs), doped with zinc (Zn-NMs) and doped with doxycycline (Dox-NMs).

Time of incubation	Number of bacteria [CFU / biofilm, expressed as mean (SD)]					
	HA	NMs	Ca-NMs	Zn-NMs	Dox-NMs	d-PTFE
12 h	3.69×10^8 (1.09×10^8)	1.28×10^8 (7.15×10^7)	2.53×10^8 (8.72×10^7)	1.19×10^8 (4.30E x10^7)	$2.98 \times 10^{6*}$ (2.62×10^6)	1.26×10^8 (7.55×10^7)
24 h	5.37×10^8 (1.87×10^8)	4.68×10^8 (2.46×10^7)	1.08×10^8 (1.57×10^7)	2.85×10^8 (1.17×10^8)	$7.42 \times 10^{6*}$ (2.52×10^6)	3.60E x10^8 (1.38×10^8)
48 h	1.14×10^9 (1.54×10^8)	3.17×10^8 (1.40×10^8)	$2.01 \times 10^{8*}$ (6.50×10^7)	6.52×10^8 (1.57×10^8)	$2.82 \times 10^{6*}$ (3.46×10^6)	3.33×10^8 (1.79×10^8)
72 h	2.59×10^8 (2.37×10^7)	4.71×10^8 (3.00×10^8)	$6.62 \times 10^{8\dagger}$ (2.09×10^8)	$8.70 \times 10^{8\dagger}$ (5.57×10^8)	1.28E x$10^{6*\dagger}$ (7.76×10^6)	1.75×10^8 (6.47×10^7)

*Statistically significant differences when compared to negative control HA discs ($p < 0.05$).
†Statistically significant differences when compared to positive control d-PTFE membranes ($p < 0.05$).

PTFE) demonstrated significantly lower counts of *A. naeslundii* when compared with the negative control group (HA discs) ($p = 0.047$). On the other hand, the counts of *F. nucleatum* were higher on control HA discs when compared to Zn-NMs, Ca-NMs and d-PTFE membranes ($p \leq 0.013$).

After 48 h, significantly higher counts of *F. nucleatum* were present on HA control biofilms, when compared with the tested membranes ($p \leq 0.001$ in all cases), except for Zn-NMs. Counts of *P. gingivalis* were significantly lower in NMs, Ca-NMs, Dox-NMs and d-PTFE, as compared to HA discs ($p \leq 0.003$). Significantly lower counts of *S. oralis*, *A. naeslundii*, *V. parvula* and *A. actinomycetemcomitan* were found on Dox-NMs when compared to the other groups ($p < 0.001$, in all cases).

After 72 h, only Dox-NMs showed significant lower counts for all tested species when compared to HA control biofilms as well as to the other groups ($p < 0.001$ in all cases). *P. gingivalis* also showed statistically significant lower counts on no doped NMs and d-PTFE membranes, when compared to the HA control biofilms ($p \leq 0.028$ in both cases).

4. Discussion

This *in vitro* investigation has shown that NMs may alter the dynamics of subgingival biofilm, especially when these NMs were doped with doxycycline, which significantly reduced the growth and accumulation of the six tested bacterial species.

The application of nanotechnology in the manufacturing of regenerative barrier membranes has demonstrated advantages, such as: i) favourable nano-mechanical properties promoting cell adhesion and proliferation, ii) a nano-topography that mimics the structure and architecture of bone [16,31,32,36] and iii) the possibility of anti-bacterial activity by the slow release of compounds with antimicrobial properties [17,37]. In this investigation, we have tested the previously reported non-resorbable polymeric nanostructured membranes [17], with a surface roughness ranging between 82.74 and 137.07 nm, what is within the desired range for osteogenic differentiation and formation of extracellular matrix [14]. These nanostructured membranes (NMs, Ca-NMs and Zn-NMs) have shown excellent cell viability [17] and due to their nanofiber diameter (300 nm), similar to that of the mineralized collagen fibres [29], have shown an enhanced absorption of proteins, such as fibronectin and vitronectin, as well as increased cell adhesion [38] an enhanced phenotypic expression of osteoblasts [38]. Furthermore, the electrospinning technique used to manufacture the tested NMs, has the potential to imitate the fibrous extracellular matrix.

The novel polymer mixture [(MMA)1-co-(HEMA)1 and (MA)3-co-(HEA)2], used in the tested membranes, is non-resorbable and biocompatible, what allows improved slow release properties when manufactured with electrospinning technology and doped with bioactive agents [26]. In this investigation, we have used antibiotic metallic cations as zinc or calcium [31,32,39,40]. The use of Ca cations has the additional advantage to potentiate bone formation, thanks to its biomimetic deposition of Ca/P, forming HA nanocrystals [15]. This fact was demonstrated in this study by the evidence of calcium salt formation by EDX. Zinc-doping of presented nanostructured membranes was also shown to favour bone formation in an *in vivo* animal model [45]. These results are consistent with those observed by Osorio et al. [16] trough the bioactivity analysis of Ca-NMs and Zn-NMs under simulated body fluid solution stating the formation of calcium/phosphate deposits.

The tested NMs membranes, doped or not, resulted in biofilms, during their exponential growth (at 12 and 24 h) phase, with lower bacterial counts, when compared to biofilms on negative control discs (HA). However, a clear antibacterial

circulation, including d-PTFE membranes (K and L), and with the external surface colonized by bacteria. After 72 h, a thick layer of bacteria could be detected. *F. nucleatum* was revelled as a key stone species, due to the formation of micro-colonies around it. The biofilm was completely mature reaching a stationary phase at that time. Only a lower bacterial density was observed in the doxycycline NMs (I and J). Magnification: (A, C, E, G, I, K) 500X; (B, D, F, H, J, L) 5000 × .

Table 2 – Number of bacteria [colony forming units (CFU)/biofilm], expressed as mean and standard deviation (SD) of *S. oralis, A. naeslundii, V. parvula, F. nucleatum, A. actinomycetemcomitans* and *P. gingivalis* grown as multi-species biofilm at the different times of incubation, measured by quantitative real-time polymerase chain reaction (qPCR) (N = 3 for each incubation time and material). Hydroxyapatite discs (HA) and dense polytetrafluoroethylene d-PTFE membranes were used as controls, and four experimental nanostructured membranes (NMs) were tested: no doped active NMs, doped with calcium (Ca-NMs), doped with zinc (Zn-NMs) and doped with doxycycline (Dox-NMs).

Bacteria	Time of incubation	Number of bacteria [CFU / biofilm, expressed as mean (SD)]					
		HA	NMs	Ca-NMs	Zn-NMs	Dox-NMs	d-PTFE
So	12	3.38×10^8 (1.35×10^8)	8.58×10^7 (6.42×10^7)	2.02×10^8 (7.43×10^7)	7.99×10^7 (4.01×10^7)	$1.19 \times 10^{5*\dagger}$ (1.88×10^4)	9.07×10^7 (6.76×10^7)
	24	3.39×10^8 (1.28×10^8)	3.01×10^8 (2.46×10^7)	1.52×10^8 (1.57×10^7)	1.88×10^8 (5.15×10^7)	$1.12 \times 10^{5*\dagger}$ (4.16×10^4)	2.26×10^8 (1.95×10^8)
	48	3.86×10^8 (1.92×10^7)	1.52×10^8 (3.09×10^7)	8.49×10^7 (6.15×10^7)	2.62×10^8 (9.26×10^7)	$1.15 \times 10^{5*\dagger}$ (9.90×10^4)	1.54×10^8 (4.45×10^7)
	72	6.14×10^7 (1.45×10^7)	1.81×10^8 (1.17×10^8)	2.85×10^8 (6.93×10^7)	3.20×10^8 (1.95×10^8)	$1.91 \times 10^{5*\dagger}$ (3.18×10^5)	8.16×10^7 (3.18×10^7)
An	12	4.20×10^5 (2.43×10^5)	1.58×10^6 (1.73×10^6)	3.70×10^6 (4.94×10^6)	1.62×10^5 (1.90×10^5)	$1.83 \times 10^{4*\dagger}$ (6.79×10^3)	2.91×10^6 (1.84×10^6)
	24	$5.76 \times 10^{6\dagger}$ (3.23×10^6)	4.36×10^6 (4.60×10^6)	2.69×10^6 (2.50×10^6)	3.37×10^6 (2.50×10^6)	$7.57 \times 10^{3*\dagger}$ (2.96×10^3)	$8.39 \times 10^{5*}$ (7.05×10^5)
	48	1.54×10^7 (5.87×10^6)	8.06×10^6 (3.05×10^6)	5.31×10^6 (1.28×10^6)	1.13×10^7 (3.33×10^6)	$1.43 \times 10^{4*\dagger}$ (9.48×10^3)	7.56×10^6 (1.04×10^6)
	72	2.89×10^6 (1.70×10^6)	3.19×10^6 (2.21×10^6)	3.40×10^6 (3.15×10^6)	6.50×10^6 (2.96×10^6)	$1.11 \times 10^{4*\dagger}$ (1.64×10^3)	2.63×10^6 (1.64×10^6)
Vp	12	1.65×10^6 (8.32×10^5)	3.17×10^6 (2.63×10^6)	4.46×10^6 (4.23×10^6)	3.27×10^6 (1.30×10^6)	$4.61 \times 10^{3*\dagger}$ (3.59×10^3	2.10×10^6 (2.31×10^6)
	24	4.60×10^6 (1.18×10^6)	1.98×10^7 (1.81×10^7)	2.87×10^6 (1.26×10^6)	3.54×10^6 (2.32×10^6)	$5.07 \times 10^{3*\dagger}$ (2.94×10^3)	7.59×10^6 (5.91×10^6)
	48	3.30×10^7 (6.12×10^6)	2.00×10^7 (1.77×10^6)	8.88×10^6 (2.94×10^6)	4.18×10^7 (1.95×10^7)	$1.53 \times 10^{4*\dagger}$ (6.17×10^3)	1.72×10^7 (1.02×10^6)
	72	1.62×10^7 (1.26×07)	2.78×10^7 (8.34×10^6)	3.78×10^7 (1.29×10^7)	3.63×10^7 (2.29×10^7)	$1.39 \times 10^{4*\dagger}$ (1.71×10^4)	1.49×10^7 (6.22×10^6)
Fn	12	1.38×10^7 (7.69×10^5)	1.50×10^7 (1.02×10^7)	2.09×10^7 (7.53×10^6)	1.67×10^7 (9.33×10^6)	$1.22 \times 10^{6*\dagger}$ (2.01×10^5)	1.17×10^7 (7.35×10^6)
	24	$1.29 \times 10^{8\dagger}$ (7.97×10^7)	5.02×10^7 (4.00×10^7)	$1.59 \times 10^{7*}$ (1.95×10^6)	$1.65 \times 10^{7*}$ (4.73×10^6)	$4.66 \times 10^{5*\dagger}$ (2.42×10^5)	$8.96 \times 10^{6*}$ (5.93×10^6)
	48	$5.68 \times 10^{8\dagger}$ (2.18×10^8)	$7.91 \times 10^{7*}$ (9.80×10^7)	$5.22 \times 10^{7*}$ (2.18×10^7)	$2.40 \times 10^{8\dagger}$ (2.19×10^7)	$3.33 \times 10^{5*\dagger}$ (2.68×10^5)	$3.39 \times 10^{7*}$ (1.18×10^7)
	72	5.23×10^7 (1.20×10^7)	2.01×10^8 (1.54×10^8)	2.40×10^8 (1.04×10^8)	$4.49 \times 10^{8*}$ (3.03×10^8)	$2.78 \times 10^{5*\dagger}$ (3.29×10^5)	4.83×10^7 (2.99×10^7)
Aa	12	1.34×10^7 (7.11×10^6)	2.00×10^7 (1.16×10^7)	2.42×10^7 (2.03×10^7)	1.87×10^7 (1.12×10^7)	$1.92 \times 10^{5*\dagger}$ (7.04×10^4)	1.87×10^7 (1.51×10^7)
	24	5.72×10^7 (2.34×10^7)	9.40×10^7 (5.76×10^7)	9.77×10^7 (9.59×10^7)	7.58×10^7 (7.22×10^7)	$1.06 \times 10^{5*\dagger}$ (6.39×10^4)	1.10×10^8 (8.38×10^7)
	48	1.36×10^8 (7.04×10^7)	5.93×10^7 (4.05×10^7)	4.77×10^7 (2.85×10^7)	1.01×108 (5.62×10^7)	$2.05 \times 10^{5*\dagger}$ (1.72×10^5)	1.21×10^8 (1.64×10^8)
	72	1.03×10^8 (1.10×10^7)	5.13×10^7 (2.68×10^7)	6.01×10^7 (4.15×10^7)	5.27×10^7 (4.53×10^7)	$1.60 \times 10^{5*\dagger}$ (1.96×10^4)	2.75×10^7 (1.33×10^7)
Pg	12	3.38×10^5 (4.03×10^4)	9.92×10^4 (4.17×10^3)	1.46×10^5 (1.03×10^4)	1.76×10^5 (1.26×10^5)	2.62×10^4 ($2.93E \times 10^4$)	1.45×10^5 (1.88×10^4)
	24	3.89×10^5 (4.88×10^4)	1.53×10^5 (6.54×10^4)	1.38×10^5 (5.12×10^5)	7.12×10^4 (1.58×10^4)	4.04×10^4 (2.51×10^4)	8.68×10^4 (1.06×10^4)
	48	$3.62 \times 10^{6\dagger}$ (9.90×10^5)	$1.59 \times 10^{5*}$ (2.29×10^5)	$4.68 \times 10^{5*}$ (2.69×10^5	1.06×10^6 (9.09×10^5)	$1.61 \times 10^{4*}$ (9.77×10^3)	$7.81 \times 10^{4*}$ (8.04×10^4)
	72	$2.36 \times 10^{7\dagger}$ (7.46×10^6)	$5.31 \times 10^{6*}$ (8.48×10^6)	$3.40 \times 10^{7\dagger}$ (4.14×10^7)	8.55×10^6 (1.42×10^7)	$8.32 \times 10^{3*\dagger}$ (1.13×10^4)	$3.23 \times 10^{5*}$ (2.57×10^5)

*Statistically significant differences when compared to negative control HA discs ($p < 0.05$).
†Statistically significant differences when compared to positive control d-PTFE membranes ($p < 0.05$).
So, Streptococcus oralis; An, *Actinomyces naeslundii*; Vp, Veillonela parvula; Fn, *Fusobacterium nucleatum*; Pg, Porphyromonas gingivalis; Aa, Aggregatibacter actinomycetemcomitans.

effect was only shown when NM were doped with antibiotics (Dox-NMs) [40–44], resulting in biofilms with significantly reduced bacterial load and counts of each of the tested bacterial species, except for *P. gingivalis*. The limited effect on *P. gingivalis* may be explained by the previously reported possible existence of antibiotic resistance genes to tetracycline or erythromycin [46]. When the biofilms reached the stationary phase (72 h), the antimicrobial effect of the NMs decreased,

especially in the group of Zn-NMs. This reduced antimicrobial activity may be due to the full coverage of the NMs surface by non-vital bacterial cells, what may prevent the likely antimicrobial effect of the nanostructured membranes. This effect has been previously described when analysing other nanostructured surfaces [17,47]. The antibacterial effect was clearly demonstrated in the membranes covered with doxycycline (Dox-NMs), an antimicrobial drug with demonstrated efficacy in the treatment of oral infections, both locally [48] as well as systemically administered [41]. This drug has shown not only antimicrobial properties, but also anti-proteolytic and anti-collagenolytic activity, through its metalloproteinase inhibiting activity [44].

In the present polymeric membranes, doxycycline adsorption is about 76.2 μg Dox per mg of membrane [50], and it is liberated for, at least, 28 days [49]. However, after this time, a significant amount of doxycycline will remain on the membrane surface. As they are non-resorbable, they may act as doxycycline coated surfaces. It can be hypothesized that membranes may exert an antibacterial effect by inhibiting the attachment and/or survival of early colonizers [17]. Moreover, Chang and Yamada (2000) [51], in a preclinical *in vivo* study on novel regenerative materials, demonstrated the effect of polyglycolic polylactic acid loaded with 25% doxycycline, showing increased new bone formation and lesser bone resorption. Similarly, Chaturvedi et al. (2008) [52] tested the effect of doping, with 25% doxycycline, resorbable membranes for periodontal regeneration, in 24 patients, and reported significant reductions in probing pocket depth and clinical attachment level gain. Other reports, however, have not validated these positive results [53,54].

The results from the present investigation lies on the importance of infection control and lack of inflammation during the early stages of wound, thus suggesting that the use of NMs, mainly when doped with antimicrobials (doxycycline) would promote periodontal and bone regeneration interventions [21–24]. However, these results should be considered cautiously due to the clear limitations of this *in vitro* investigation, such as the use of only six bacterial species in the tested biofilm model and the lack of host response evaluation, what indicate the need for further research, especially *in vivo* experimental studies using histological outcomes to clearly assess their impact in promoting periodontal or bone regeneration.

5. Conclusions

Within the limitations of this *in vitro* study, it can be concluded that nanostructured membranes were able to alter the kinetics and development of the formation of *in vitro* biofilms, when compared to the formation on control hydroxyapatite discs. Specifically, doxycycline-doped nanostructured membranes had a significant impact in the counts of *S. oralis*, *V. parvula*, *A. naeslundii*, *F. nucleatum*, *A. actinomycetemcomitans* and *P. gingivalis* in a validated *in vitro* subgingival biofilm model.

Acknowledgements

The project MAT2017-85999-P was supported by the Ministry of Economy and Competitiveness and European Regional Development Fund. The participation of María Sánchez was funded by Extraordinary Chair DENTAID in Periodontal Research (University Complutense). The participation of Jaime Bueno was funded by a predoctoral contract (CT42/18-CT43/18) by University Complutense of Madrid. Microscopy analyses were carried out at the Centre of Microscopy and Cytometry, University Complutense of Madrid, Spain.

Appendix A. Supplementary data

Supplementary material related to this article can be found, in the online version, at doi:https://doi.org/10.1016/j.dental.2020.09.011.

REFERENCES

[1] Papapanou PN, Sanz M, Buduneli N, Dietrich T, Feres M, Fine DH, et al. Periodontitis: consensus report of workgroup 2 of the 2017 world workshop on the classification of periodontal and peri-implant diseases and conditions. J Clin Periodontol 2018;45(Suppl 20):S162–S170.
[2] Kassebaum NJ, Bernabé E, Dahiya M, Bhandari B, Murray CJL, Marcenes W. Global burden of severe periodontitis in 1990-2010. J Dental Res 2014;93:1045–53.
[3] Cunha-Cruz J, Hujoel PP, Kressin NR. Oral health-related quality of life of periodontal patients. J Periodontal Res Suppl 2007;42:169–76.
[4] Monsarrat P, Blaizot A, Kemoun P, Ravaud P, Nabet C, Sixou M, et al. Clinical research activity in periodontal medicine: a systematic mapping of trial registers. J Clin Periodontol 2016;43:390–400.
[5] Hansen GM, Egeberg A, Holmstrup P, Hansen PR. Relation of periodontitis to risk of cardiovascular and all-cause mortality (from a danish nationwide cohort study). Am J Cardiol 2016;118:489–93.
[6] Socransky SS, Haffajee AD. Periodontal microbial ecology. Periodontol 2000 2005;38:135–87.
[7] Kolenbrander PE, Palmer RJ, Rickard AH, Jakubovics NS, Chalmers NI, Diaz PI. Bacterial interactions and successions during plaque development. Periodontol 2000 2006;42:47–79.
[8] Page RC, Kornman KS. The pathogenesis of human periodontitis: an introduction. Periodontol 2000 1997;14:9–11.
[9] Kinane DF, Attström R, EWiPg B. Advances in the pathogenesis of periodontitis. Group B consensus report of the fifth European Workshop in Periodontology. J Clin Periodontol 2005;32(Suppl 6):130–1.
[10] Heitz-Mayfield LJA, Trombelli L, Heitz F, Needleman I, Moles D. A systematic review of the effect of surgical debridement vs non-surgical debridement for the treatment of chronic periodontitis. J Clin Periodontol 2002;29(Suppl 3):92–102,; discussion 60-2.
[11] Ramfjord SP, Caffesse RG, Morrison EC, Hill RW, Kerry GJ, Appleberry EA, et al. 4 modalities of periodontal treatment compared over 5 years. J Clin Periodontol 1987;14:445–52.
[12] Becker W, Becker BE, Caffesse R, Kerry G, Ochsenbein C, Morrison E, et al. A longitudinal study comparing scaling, osseous surgery, and modified widman procedures: results after 5 years. J Periodontol 2001;72:1675–84.
[13] Ramseier CA, Rasperini G, Batia S, Giannobile WV. Advanced reconstructive technologies for periodontal tissue repair. Periodontol 2000 2012;59:185–202.
[14] Bruzauskaite I, Bironaite D, Bagdonas E, Bernotiene E. Scaffolds and cells for tissue regeneration: different scaffold

pore sizes-different cell effects. Cytotechnology 2016;68:355–69.
[15] Osorio R, Alfonso-Rodríguez CA, Medina-Castillo AL, Alaminos M, Toledano M. Bioactive polymeric nanoparticles for periodontal therapy. PLoS One 2016;11:e0166217.
[16] Osorio R, Alfonso-Rodríguez CA, Osorio E, Medina-Castillo AL, Alaminos M, Toledano-Osorio M, et al. Novel potential scaffold for periodontal tissue engineering. Clin Oral Investig 2017;21:2695–707.
[17] Sanchez MC, Toledano-Osorio M, Bueno J, Figuero E, Toledano M, Medina-Castillo AL, et al. Antibacterial effects of polymeric PolymP-n Active nanoparticles. An in vitro biofilm study. Dent Mater 2019;35:156–68.
[18] Listgarten MA, Rosenberg MM. Histological study of repair following new attachment procedures in human periodontal lesions. J Periodontol 1979;50:333–44.
[19] Melcher AH. On the repair potential of periodontal tissues. J Periodontol 1976;47:256–60.
[20] Karring T, Isidor F, Nyman S, Lindme J. New attachment formation on teeth with a reduced but healthy periodontal ligament. J Clin Periodontol 1985;12:51–60.
[21] Nowzari H, Slots J. Microorganisms in polytetrafluoroethylene barrier membranes for guided tissue regeneration. J Clin Periodontol 1994;21:203–10.
[22] Nowzari H, Matian F, Slots J. Periodontal pathogens on polytetrafluoroethylene membrane for guided tissue regeneration inhibit healing. J Clin Periodontol 1995;22:469–74.
[23] Machtei EE, Dunford RG, Norderyd OM, Zambon JJ, Genco RJ. Guided Tissue Regeneration and Anti-Infective Therapy in the Treatment of Class II Furcation Defects. J Clin Periodontol 1993;64:968–73.
[24] Selvig KA, Kersten BG, Chamberlain ADH, Wikesjö UME, Nilvúus RE. Regenerative surgery of intrabony periodontal defects using ePTFE barrier membranes: scanning Electron microscopic evaluation of retrieved membranes versus clinical healing. J Periodontol 1992;63:974–8.
[25] Bartold PM, Gronthos S, Ivanovski S, Fisher A, Hutmacher DW. Tissue engineered periodontal products. J Periodontal Res Suppl 2016;51:1–15.
[26] Feuser PE, Gaspar PC, Ricci-Júnior E, MCSd Silva, Nele M, Sayer C, et al. Synthesis and Characterization of Poly(Methyl Methacrylate) PMMA and Evaluation of Cytotoxicity for Biomedical Application. Macromol Symp 2014;343: 65–9.
[27] Sariibrahimoglu K, Yang W, Leeuwenburgh SC, Yang F, Wolke JG, Zuo Y, et al. Development of porous polyurethane/strontium-substituted hydroxyapatite composites for bone regeneration. J Biomed Mater Res A 2015;103:1930–9.
[28] Toledano M, Osorio E, Aguilera FS, Muñoz-Soto E, Toledano-Osorio M, López-López MT, et al. Polymeric nanoparticles for endodontic therapy. J Mech Behav Biomed Mater 2020;103.
[29] Ma PX. Biomimetic materials for tissue engineering. Adv Drug Deliv Rev 2008;60:184–98.
[30] Bottino MC, Thomas V, Janowski GM. A novel spatially designed and functionally graded electrospun membrane for periodontal regeneration. Acta Biomater 2011;7:216–24.
[31] Munchow EA, Pankajakshan D, Albuquerque MT, Kamocki K, Piva E, Gregory RL, et al. Synthesis and characterization of CaO-loaded electrospun matrices for bone tissue engineering. Clin Oral Investig 2016;20:1921–33.
[32] Augustine R, Malik HN, Singhal DK, Mukherjee A, Malakar D, Kalarikkal N, et al. Electrospun polycaprolactone/ZnO nanocomposite membranes as biomaterials with antibacterial and cell adhesion properties. J Polym Res 2014;21.
[33] Pascale D, Gordon J, Lamster I, Mann P, Seiger M, Arndt W. Concentration of doxycycline in human gingival fluid. J Clin Periodontol 1986;13:841–4.
[34] Kaur K, Sikri P. Evaluation of the effect of allograft with doxycycline versus the allograft alone in the treatment of infrabony defects: a controlled clinical and radiographical study. Dent Res J (Isfahan) 2013;10:238–46.
[35] Sanchez MC, Llama-Palacios A, Fernandez E, Figuero E, Marin MJ, Leon R, et al. An in vitro biofilm model associated to dental implants: structural and quantitative analysis of in vitro biofilm formation on different dental implant surfaces. Dent Mater 2014;30:1161–71.
[36] Münchow EA, Albuquerque MTP, Zero B, Kamocki K, Piva E, Gregory RL, et al. Development and characterization of novel ZnO-loaded electrospun membranes for periodontal regeneration. Dental Mater 2015;31:1038–51.
[37] Repanas A, Andriopoulou S, Glasmacher B. The significance of electrospinning as a method to create fibrous scaffolds for biomedical engineering and drug delivery applications. Int J Drug Deliv Technol 2016;31:137–46.
[38] Woo KM, Chen VJ, Ma PX. Nano-fibrous scaffolding architecture selectively enhances protein adsorption contributing to cell attachment. J Biomed Mater Res A 2003;67:531–7.
[39] Bottino MC, Arthur RA, Waeiss RA, Kamocki K, Gregson KS, Gregory RL. Biodegradable nanofibrous drug delivery systems: effects of metronidazole and ciprofloxacin on periodontopathogens and commensal oral bacteria. Clin Oral Investig 2014;18:2151–8.
[40] Monteiro AP, Rocha CM, Oliveira MF, Gontijo SM, Agudelo RR, Sinisterra RD, et al. Nanofibers containing tetracycline/beta-cyclodextrin: Physico-chemical characterization and antimicrobial evaluation. Carbohydr Polym 2017;156:417–26.
[41] Graziani F, Karapetsa D, Alonso B, Herrera D. Nonsurgical and surgical treatment of periodontitis: how many options for one disease? Periodontol 2000 2017;75:152–88.
[42] van Winkelhoff AJ, Gonzales DH, Winkel EG, Dellemijn-Kippuw N, Vandenbroucke-Grauls CMJE, Sanz M. Antimicrobial resistance in the subgingival microflora in patients with adult periodontitis. J Clin Periodontol 2000;27:79–86.
[43] Rodrigues RM, Goncalves C, Souto R, Feres-Filho EJ, Uzeda M, Colombo AP. Antibiotic resistance profile of the subgingival microbiota following systemic or local tetracycline therapy. J Clin Periodontol 2004;31:420–7.
[44] Golub LM, Ramamurthy N, McNamara TF, Gomes B, Wolff M, Casino A, et al. Tetracyclines inhibit tissue collagenase activity. J Periodontal Res Suppl 1984;19:651–5.
[45] Toledano M, Gutierrez-Perez JL, Gutierrez-Corrales A, Serrera-Figallo MA, Toledano-Osorio M, Rosales-Leal JI, et al. Novel non-resorbable polymeric-nanostructured scaffolds for guided bone regeneration. Clin Oral Investig 2019.
[46] Sanai Y, Persson GR, Starr JR, Luis HS, Bernardo M, Leitao J, et al. Presence and antibiotic resistance of Porphyromonas gingivalis, Prevotella intermedia, and Prevotella nigrescens in children. J Clin Periodontol 2002;29:929–34.
[47] Schacht VJ, Neumann LV, Sandhi SK, Chen L, Henning T, Klar PJ, et al. Effects of silver nanoparticles on microbial growth dynamics. J Appl Microbiol 2013;114:25–35.
[48] Matesanz-Perez P, Garcia-Gargallo M, Figuero E, Bascones-Martinez A, Sanz M, Herrera D. A systematic review on the effects of local antimicrobials as adjuncts to subgingival debridement, compared with subgingival debridement alone, in the treatment of chronic periodontitis. J Clin Periodontol 2013;40:227–41.
[49] Toledano-Osorio M, Babu JP, Osorio R, Medina-Castillo AL, Garcia-Godoy F, Toledano M. Modified polymeric

nanoparticles exert in vitro antimicrobial activity against oral Bacteria. Materials (Basel) 2018;11.
[50] Osorio R, Carrasco-Carmona A, Toledano M, Osorio E, Medina-Castillo AL, Iskandar L, et al. *Ex vivo* investigations on bioinspired electrospun membranes as potential biomaterials for bone regeneration. J Dent 2020;98:103359.
[51] Chang C-Y, Yamada S. Evaluation of the regenerative effect of a 25% doxycycline-loaded biodegradable membrane for guided tissue regeneration. J Periodontol 2000;71:1086–93.
[52] Chaturvedi R, Gill AS, Sikri P. Evaluation of the regenerative potential of 25% doxycycline-loaded biodegradable membrane vs biodegradable membrane alone in the treatment of human periodontal infrabony defects: a clinical and radiological study. Indian J Dent Res 2008;19:116–23.
[53] Eickholz P, Rollke L, Schacher B, Wohlfeil M, Dannewitz B, Kaltschmitt J, et al. Enamel matrix derivative in propylene glycol alginate for treatment of infrabony defects with or without systemic doxycycline: 12- and 24-month results. J Periodontol 2014;85:669–75.
[54] Agarwal A, Gupta ND. Combination of bone allograft, barrier membrane and doxycycline in the treatment of infrabony periodontal defects: A comparative trial. Saudi Dent J 2015;27:155–60.